

# Pulsed laser CVD investigations of single-wall carbon nanotube growth dynamics

Z. Liu · D.J. Styers-Barnett · A.A. Puretzky · C.M. Rouleau · D. Yuan · I.N. Ivanov · K. Xiao · J. Liu · D.B. Geohegan

Received: 12 October 2007 / Accepted: 9 April 2008 / Published online: 17 July 2008  
© Springer-Verlag 2008

**Abstract** The nucleation and rapid growth of single-wall carbon nanotubes (SWNTs) were explored by pulsed-laser assisted chemical vapor deposition (PLA-CVD). A special high-power, Nd:YAG laser system with tunable pulse width ( $>0.5$  ms) was implemented to rapidly heat ( $>3 \times 10^4$  °C/s) metal catalyst-covered substrates to different growth temperatures for very brief (sub-second) and controlled time periods as measured by in situ optical pyrometry. Utilizing growth directly on transmission electron microscopy grids, exclusively SWNTs were found to grow under rapid heating conditions, with a minimum nucleation time of  $>0.1$  s. By measuring the length of nanotubes grown by single laser pulses, extremely fast growth rates (up to 100 microns/s) were found to result from the rapid heating and cooling induced by the laser treatment. Subsequent laser pulses were found not to incrementally continue the growth of these nanotubes, but instead activate previously inactive catalyst nanoparticles to grow new nanotubes. Localized growth of nanotubes with variable density was demonstrated through this process and was applied for the reliable direct-write synthesis of SWNTs onto pre-patterned, catalyst-covered metal electrodes for the synthesis of SWNT field-effect transistors.

**PACS** 81.07.De · 85.35.Kt · 61.48.De · 81.16.Mk

## 1 Introduction

Because the electronic and optical properties of carbon nanotubes depend sensitively on tube structure, a major goal in nanotube production is to control growth with predefined structure and functionality [1, 2]. This requires both a detailed understanding of SWNT nucleation and growth kinetics as well as identification of the salient processing parameters for selective growth of SWNTs. Theoretical studies on the nucleation and growth mechanism predicate that once the nanotube nuclei are formed, growth should proceed through further incorporation of carbon at the catalyst-tube interface [3, 4]. Thus, the initial growth of SWNTs can strongly affect the resulting nanotube structure in terms of chirality, diameter, length, and physical properties. Despite their importance, many of these fundamental questions remain unanswered. Over what timescales do nanotubes nucleate and is nucleation uniform across a heated sample? What are the growth rates for carbon nanotubes and why does growth terminate? Can it be restarted with subsequent processing? This paper attempts to address these questions by applying well-defined laser pulses as the heat source for CVD to understand the kinetics of nucleation and growth of nanotubes formed under rapid laser heating.

Due to the limited availability of techniques to probe these processes, few experimental studies of the nucleation and growth of SWNTs have been performed [5–10]. Recently, the initial growth of CNTs has been experimentally investigated by in-situ high-resolution transmission electron microscopy (TEM) [5–7]. However, the vacuum apparatus of TEM chamber applies significant restrictions on the growth conditions, resulting in carbon nanotubes with

---

Z. Liu · D.J. Styers-Barnett · A.A. Puretzky · C.M. Rouleau · I.N. Ivanov · K. Xiao · D.B. Geohegan (✉)  
Center for Nanophase Materials Sciences, Oak Ridge National Laboratory, Oak Ridge, TN 37831-6031, USA  
e-mail: [odg@ornl.gov](mailto:odg@ornl.gov)

C.M. Rouleau · A.A. Puretzky · D.B. Geohegan  
Materials Science and Technology Division, Oak Ridge National Laboratory, Oak Ridge, TN 37831-6056, USA

D. Yuan · J. Liu  
Department of Chemistry, Duke University, Durham, NC 27708, USA

very low initial growth rates ( $\sim 0.3$  nm/s) and long nucleation times ( $\sim 50$  s) as compared with other approaches [5]. Futaba and Zhu et al. [9, 10] used a simple equation to describe the time evolution of SWNT forest growth and plotted out the initial growth rate about 1–2  $\mu\text{m/s}$ . However, these rates only apply for the specific geometry of vertically-aligned carbon nanotube forests on the minute time scale.

One major experimental limitation is the inability to sufficiently limit growth time to understand how and when nucleation and growth can occur. Using a technique involving rapid substrate insertion into a hot CVD furnace (with a heating time of several seconds), Huang et al. [11] first reported that fast heating is favored for the growth of long nanotubes. However the exact timescales for nucleation and the dynamics of the initial growth rates could not be measured. Here, pulsed laser heating is used to produce sub-second growth times to study the kinetics of carbon nanotube nucleation and growth under typical CVD conditions and on timescales relevant to standard growth processes. With pulsed laser-assisted chemical vapor deposition (PLA-CVD), much higher thermal ramping rates and more precisely controlled sustained substrate heating times can be explored as compared to conventional CVD processes. Pulsed laser heating therefore permits exploration of both the initial dynamics of nanotube formation and early time growth as well as longer term questions regarding sustained nucleation and incremental growth.

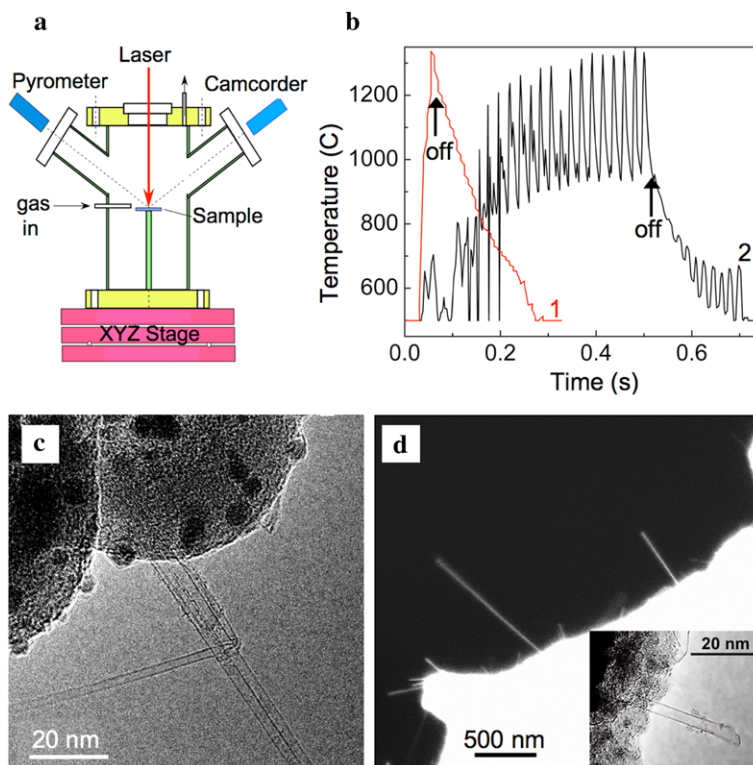
PLA-CVD utilizes control over the laser pulse width, intensity, repetition rate, and number of pulses to regu-

late heating of the sample. “On-off” switching of the heat source on the millisecond timescale permits sub-second investigations of the growth kinetics. Recently, a few research groups have reported the feasibility of using laser CVD to synthesize carbon nanotubes using cw lasers as heating sources [12–15]. In these works, however, the focus has been to demonstrate the ability to produce tubes (both single- and multi-wall) in localized regions or to optimize the growth conditions for general quality. Here, in addition to exploration of localized nanotube growth for direct-write device applications, millisecond pulse laser heating is used to explore fundamental mechanisms of SWNT growth by CVD, including the possibility of re-growth and re-nucleation under repeated laser heating.

## 2 Experimental

The specially-designed (PLA-CVD) system used here consists of four parts (Fig. 1a): (1) a high power, pulsed laser system (Nd:YAG,  $\lambda = 1064$  nm, 600 W maximum average power, 1–500 Hz repetition rate, 0.5–50 ms pulse width, 3 mm focused spot size); (2) a windowed CVD reaction chamber mounted on a 3-axis translation stage; (3) pre-mixed gas supply; and (4) a temperature monitoring system including a computer-controlled, in situ, two-color optical pyrometer with 2 ms temporal and  $\sim 2$  mm spatial resolution with a temperature range of 500–2300°C. Additionally, substrate heating is video monitored.

**Fig. 1** (a) Schematic of PLA-CVD vacuum chamber. (b) Time-dependent temperature profile of a 1 cm<sup>2</sup> Si/SiO<sub>2</sub> wafer irradiated by a single 50 ms laser pulse (1) and a Mo TEM grid from 25 pulses of 5 ms width (2). Arrows show the time when laser irradiation is terminated. (c) TEM image of CNTs grown on a Mo grid coated with 1 nm Fe/Al<sub>2</sub>O<sub>3</sub> by 1500 laser pulses. (d) SEM of nanotubes grown using 20 pulses on an identically prepared grid as (c). *Inset* shows a TEM image of the end of a nanotube free of catalyst particle



Carbon nanotube synthesis was carried out on Si/SO<sub>2</sub> wafers and Mo TEM grids coated with either 1 nm Fe/10 nm Al<sub>2</sub>O<sub>3</sub> thin films or ferritin catalyst nanoparticles, using feedstock gases (800 sccm methane/200 sccm ethylene) in a background of 2000 sccm of Ar and 500 sccm of H<sub>2</sub>. Atmospheric pressure was used in all experiments. Characterization of the samples was performed by SEM (Hitachi, S4700), HRTEM (Hitachi HF-2000), Raman (Renishaw 1000) and AFM (Dimension, 3100) to examine the length, diameter, number of walls, and nanotube defect level and abundance of the nanotube products.

### 3 Results and discussion

In order to investigate nucleation and growth rates of CVD grown carbon nanotubes, PLA-CVD experiments were performed with both single laser pulses and pulse trains. In addition to these studies, sets of “macropulses” were used to investigate the possibility of restarting or re-nucleating growth after well-defined time intervals. Finally, direct-writing of SWNT transistors onto pre-patterned catalyst-coated electrode structures by localized pulsed laser CVD is presented.

#### 3.1 Nucleation studies

Heating of silicon substrates with variable temperature profiles can be achieved using pulse trains consisting of overlapping pulses at a repetition rate of 50 Hz. Thermal ramping rates of 5000°C/s can be achieved using pulse energies of 1 J/pulse, 50 Hz, 5 ms. By applying a specific number of laser pulses and characterizing the resulting growth by Raman spectroscopy and electron microscopy, the minimum time necessary for nanotube nucleation was investigated. Figures 1c, d show TEM and SEM images from 1 J/pulse irradiated Mo grids coated with Fe/Al<sub>2</sub>O<sub>3</sub> catalyst after 1500 (c) and 20 (d) pulses. For longer growth times (500 pulses and higher), bundles of 3–5 nanotubes are observed (Fig. 1c). For shorter pulse trains ( $\leq 250$  pulses), only individual tubes are seen by TEM (Fig. 1d, inset). Irradiation with 10 pulses (0.2 s) generated no observable nanotubes. From the electron microscopy study it can be determined that the first nanotube nucleation occurs within the first half second, but that between 10 and 20 heat pulses are required to generate measurable growth. Furthermore, in the first few seconds of growth, the nucleation density is insufficient to generate bundles. Investigation of the pyrometry data provides insight to the timescales for the nucleation process.

Figure 1b shows the temperature profile (line 2) of a 2000-mesh Mo TEM grid irradiated with 25 laser pulses (0.5 s of laser illumination). The optimum temperature for SWNT growth under these conditions in traditional furnace

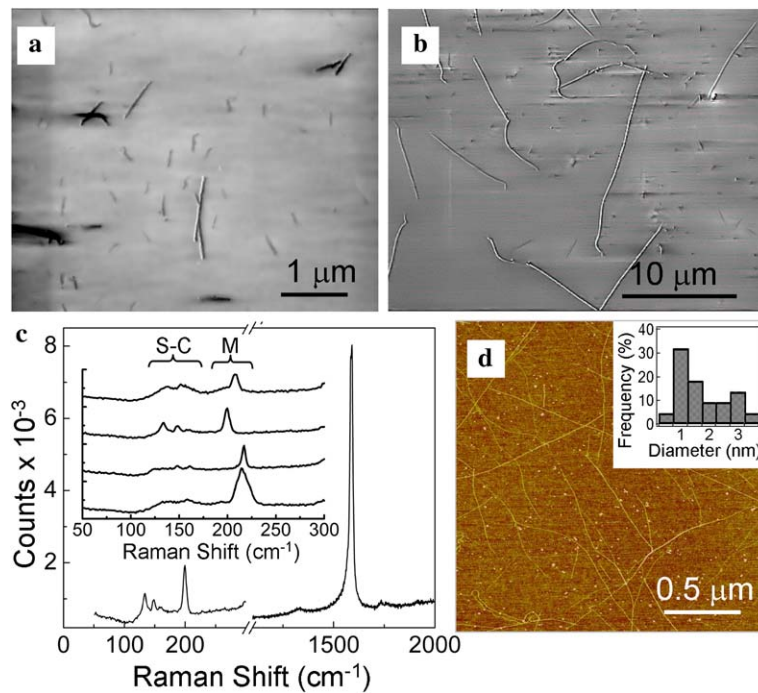
CVD is typically 900°C, thus the actual SWNT growth time is defined as the duration when the sample temperature is above this threshold [11, 16]. The temperature profile corresponding to the 20 pulse experiment shows that the sample spends 0.2 seconds with an average temperature above the nanotube growth temperature. However, at 1 J/pulse, the laser pulse creates large fluctuations in the temperature ( $\pm 150^\circ\text{C}$ ) upon each shot, making an absolute measure of the nucleation time and growth rates difficult.

In order to eliminate the oscillating temperature effects of the multi pulse experiments, a single, 50 ms laser pulse has been used for nanotube nucleation and growth investigations. A typical time-dependent temperature profile of the irradiated area of a silicon substrate heated by a single laser pulse with 50 ms width, 52 J/pulse is seen in Fig. 1b (line 1). This high energy single pulse generates ramping rates  $\sim 3.3 \times 10^4$ °C/s, bringing the sample to 900°C within 25 ms. Once the laser pulse ends, the temperature drops to 500°C within 0.25 s. This temperature profile is very reproducible from one sample to the next for a given laser pulse width, energy, and substrate size. SEM investigations of these samples (Figs. 2a, b) reveal that nanotubes can be nucleated and grown using a single laser pulse. In this single pulse laser irradiation regime, the actual growth time, using the threshold temperature described above, is 0.10 s, representing the minimum observed nucleation time for carbon nanotubes.

It should be noted that only single-wall nanotubes and SWNT bundles are grown from these catalysts using PLA-CVD, in contrast to the formation of multi-walled carbon nanotubes (MWNTs)/SWNTs mixtures typically grown using tube-furnace thermal CVD methods for the same growth conditions. This has been confirmed by TEM, AFM, and micro Raman spectroscopy with a laser excitation of 632.8 nm [90 individual nanotubes] (Figs. 2c, d). The Raman results clearly show the G-band and radial breathing modes (RBM) of SWNTs with diameters of 1–3 nm, as calculated from the relation between RBM frequency and diameter described by Jorio et al. ( $\omega_{\text{RBM}} = 248 \text{ cm}^{-1}/d_t$ , where  $\omega_{\text{RBM}}$  is the Raman shift of the RBM, and  $d_t$  is the tube diameter) [17]. Several tubes are excited within the diameter of the Raman laser beam, giving rise to the congested RBM region. The two regions marked S-C and M correspond to the semiconducting and metallic tube modes, respectively. Topographic height measurements from AFM (Fig. 2d) further confirm the presence of individual SWNTs or small bundles, yielding a diameter distribution centered at 1.5 nm.

It is possible that fast local heating generated in PLA-CVD creates a preferential growth environment for SWNTs over MWNTs. According to the nanotube growth model detailed elsewhere [18, 19], SWNTs should grow preferentially at relatively high temperatures, e.g.,  $> 700^\circ\text{C}$  [18]. However, in a typical furnace CVD, poisoning of catalyst

**Fig. 2** (a) and (b) SEM of nanotubes grown from a single 50 ms laser pulse (52 J) using Fe/Al<sub>2</sub>O<sub>3</sub> thin film and ferritin catalysts, respectively. (c) Typical Raman spectrum of SWNTs grown using Fe/Al<sub>2</sub>O<sub>3</sub> thin film on Si, inset shows the radial breathing modes of SWNT collected from different areas of the same sample. S-C is the semiconducting region, M is metallic. (d) AFM image of SWNTs produced using 6000 laser pulses (5 ms, 50 Hz, 0.5 J/pulse). *Inset* shows the diameter distribution of SWNTs



nanoparticles occurs at high temperatures that sharply terminates the growth as the temperature increases. The high temperature poisoning could include chemical modification of catalyst nanoparticles, e.g., due to reactions with the ambient gases or catalyst modification by gas phase pyrolysis products [18]. The localized surface heating in laser CVD could completely change the kinetics of these processes, resulting in increase of the upper growth temperature. In addition, in pulsed laser CVD, the catalyst particles are rapidly cycled from low temperature to high and back to low again, which will transiently affect carbon solubility and the surface chemistry of the nanoparticles. The end result is a process that can produce nanotubes at a higher temperature which, according to our model [19], favors single walled structures with rapid growth rates.

### 3.2 Growth rates

The growth from Fe/Al<sub>2</sub>O<sub>3</sub> catalyst thin films using the single laser pulse described in the previous section yields nanotubes/bundles with a typical length of 1 μm (Fig. 2a) for a growth time of 0.1 s. This gives an average initial growth rate of 10 μm/s, much higher than the fastest value reported using conventional CVD methods (3.3 μm/s) [11]. Furthermore, ~10 μm-long carbon nanotubes were grown from a single laser pulse using discrete catalytic ferritin nanoparticles, resulting in an estimated growth rate of 100 μm/s (Fig. 2b). This is the fastest initial growth rate observed and reported to date. These very high growth rates may be associated with the rapid heating rates obtained by PLA-CVD. Indeed, according to our models [18, 19],

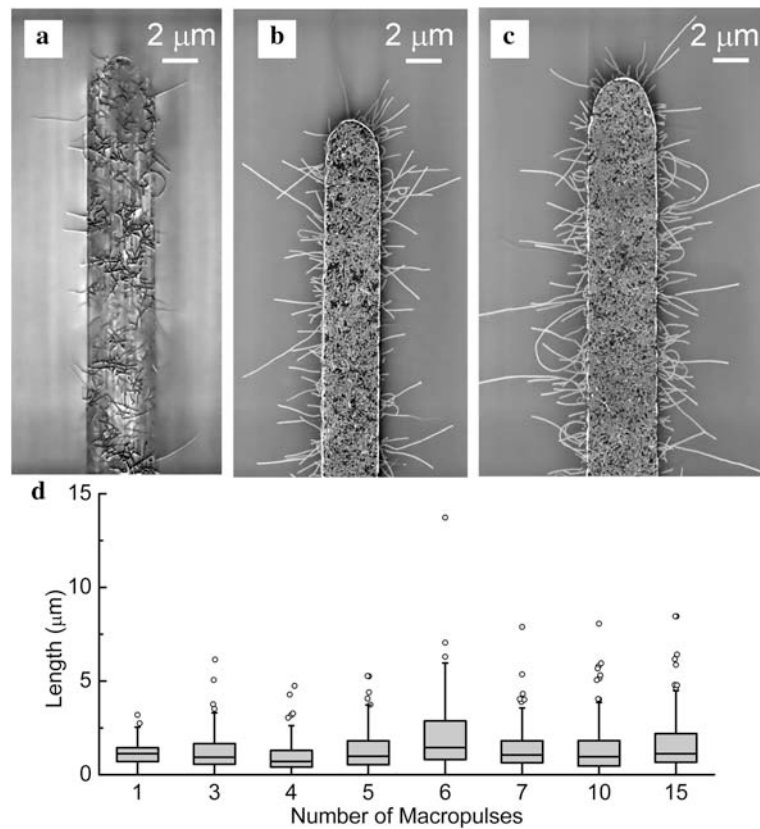
the growth rate should increase rapidly as the temperature increases, but experimentally the growth rate follows the theory only at relatively low temperatures because of the high temperature poisoning of catalyst nanoparticles discussed above. Pulsed laser heating could lead to suppression of the high temperature poisoning and the rapid increase of the growth rate according to the theoretical predictions [18, 19].

While single pulse laser heating enables ultra high growth rates for nanotubes from both Fe/Al<sub>2</sub>O<sub>3</sub> thin film and ferritin catalysts, there are substantial differences in the growth rates measured from the two different catalysts. This may be associated with differences in how the catalyst surface is prepared, and the growth mechanism associated with the different catalyst morphologies. For thin film catalysts, Fe nanoparticles are embedded in an Al<sub>2</sub>O<sub>3</sub> film, which leads to base-growth (see TEM image in Fig. 1d). On the other hand, discrete ferritin nanoparticles on a smooth Si surface are highly mobile at elevated temperatures, possibly resulting in tip-growth, which has been observed in other studies using ferritin [11, 16].

### 3.3 Incremental growth

A repetitive laser pulse sequence was used to investigate the nucleation and growth at longer times. Samples were repeatedly irradiated with 200 shot macropulses (5 ms/pulse, 0.5 J/pulse, 50 Hz) separated by 10 seconds. This pulse train raises the substrate temperature above 900°C on every macropulse, and the 10 second separation is sufficient to

**Fig. 3** (a–c) SEM images of nanotubes grown on patterned substrates using 1, 5, and 15 macropulses, respectively. (d) Statistics of nanotube length as a function of number of macropulses applied. The horizontal line is the median length for each growth experiment. Boxes and lines include 50% and ~90% of the measured tubes, respectively, while the open circles are outliers



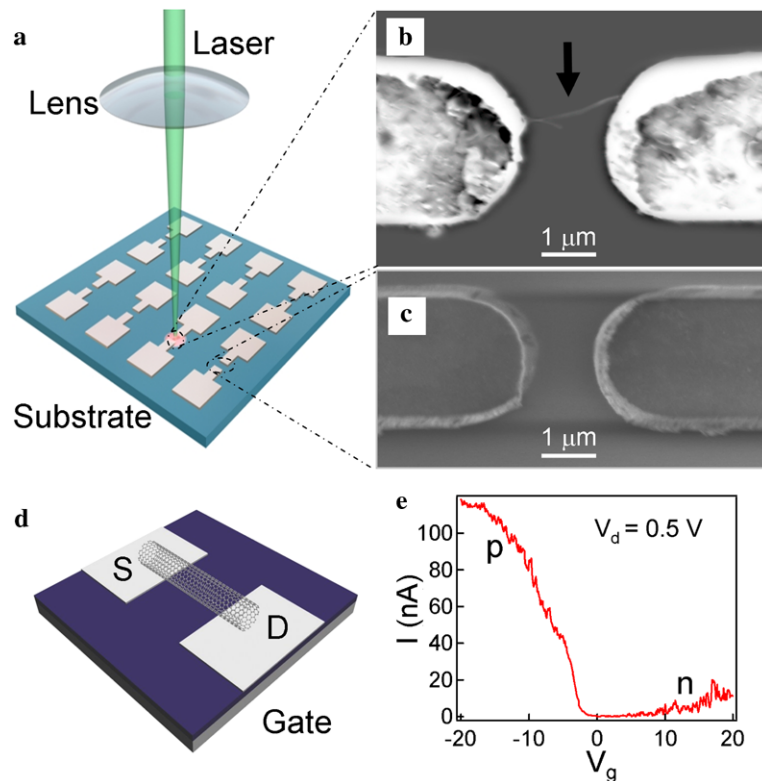
completely cool the sample between irradiation steps to ensure growth and nucleation stops. In order to better assess nanotube growth and density, the Fe/Al<sub>2</sub>O<sub>3</sub> catalyst thin films were patterned in 3 micron wide and several microns-long bands. Samples were irradiated with increasing numbers of macropulses, and the density and length of nanotubes for each step was measured. Figure 3 shows the resulting nanotube growth for 1 to 15 macropulses. The SEM data (Figs. 3a–c) reveals an increase in the density of tubes, but careful assessment of the median length (Fig. 3d) shows no statistically significant increase. In Fig. 3d, the boxes and lines include 50% and ~90% of the measured tubes, respectively, while the open circles are outliers. No incremental growth or restart of the growth is observed, but new tubes are nucleated for the entire experiment (several minutes) during each macropulse. Therefore we conclude that once growth from a particular catalyst particle has terminated, growth cannot be resumed, but as mentioned above, the rapid thermal cycling allows new catalytic sites to be activated on subsequent laser pulses. Comparable with nucleation rates in conventional CVD, only a small fraction of the nanoparticles nucleate a nanotube per laser shot.

### 3.4 Direct-writing SWNT devices

To assess the SWNT suitability for device applications, single SWNT transistors were fabricated by localized laser irra-

diation growth. Carbon nanotube field effect transistors were made by fabricating pre-defined electrodes of 5 nm Ti and 80 nm Au with 1 nm Fe/10 nm Al<sub>2</sub>O<sub>3</sub> catalyst thin film using photolithography. Figure 4a illustrates the process of direct writing of SWNTs onto pre-fabricated source/drain contacts. Successive PLA-CVD growth events were attempted to bridge the two electrodes with a carbon nanotube. *I*–*V* measurements were performed by applying a bias to the drain electrode and using the silicon substrate as a back gate (see Fig. 4d). The electrical measurements were carried out using a semiconductor parameter analyzer (Agilent 4156B). An in-situ contacted SWNT was produced inside the local hot zone, shown in Fig. 4b. In comparison, no nanotube growth occurred at adjacent electrodes outside the heating zone (see Fig. 4c). The controllable yield and ability to nucleate nanotubes on subsequent laser pulses permits the growth of individual SWNTs between two electrodes, while the short growth time substantially reduces the risk of thermal damage to the pre-defined metal electrodes. All the devices exhibited a resistance between 100–400 kΩ, comparable to the results of post-CVD contacted SWNTs [20]. Around 70% of the resulting SWNT transistors exhibited pronounced ambipolar transport characteristics with on/off ratios up to 1000 (shown in Fig. 4e). The beam can be focused to a micron-sized spot, offering possibilities to direct-write SWNT devices at very high density.

**Fig. 4** (a) Schematic of local direct-writing of SWNTs for device applications. (b) An in-situ contacted nanotube bridging two electrodes. Arrow identifies the nanotube. (c) No nanotube growth from adjacent electrodes outside the heating zone. (d) Schematic diagram of a back-gated SWNT field-effect transistor. (e)  $I-V_g$  curve of the transistor exhibiting ambipolar behavior.  $V_{ds} = 0.5$  V



#### 4 Summary

Pulsed laser heating has been used to investigate the dynamics of nucleation and initial growth of carbon nanotubes by chemical vapor deposition. Nucleation and growth has been shown to result from a single 50 ms laser pulse or upon heating with a 50 Hz pulse train of 5 ms pulses. Exclusively single wall nanotubes and SWNT bundles were observed for all nanotubes investigated by TEM in this study. The independent measurements of individual tubes by TEM, AFM, and Raman spectroscopy show single walled structures with an average diameter of 1.5 nm. The rapid heating rates (up to  $3.3 \times 10^4$  °C/s) and “cold” environment of PLA-CVD may lead to the preferential formation of single walled tubes over multiwall structures. Measurements of the minimum nucleation time have shown nanotube formation in 0.1 seconds, with continued nucleation of new tubes occurring over at least 30 seconds. The nucleation efficiency is comparable to that of traditional CVD. Extremely high initial growth rates of  $10 \mu\text{m/s}$  using thin film catalysts and up to  $100 \mu\text{m/s}$  using ferritin nanoparticles were measured under single pulse heating. No incremental or re-growth of existing tubes upon subsequent irradiation has been observed with this technique, but subsequent laser pulses do initiate nucleation and growth of new nanotubes on a given catalyst film. Through spatial and temporal control of the laser focus, direct in-situ writing of SWNTs field-effect transistors onto pre-defined electrodes was demonstrated. The PLA-

CVD technique is a powerful tool to investigate the fundamental mechanisms of nanotube formation and growth, as well as offering a promising method for localized growth of SWNTs for device applications.

**Acknowledgements** We gratefully thank Dr. Daihua Zhang, Dr. Xiaolei Liu at USC, Dr. Weidong Luo, Dr. Gyula Eres, Dr. Zhixian Zhou, and Dr. Jing Tao at ORNL for helpful discussion on this manuscript. The authors acknowledge the technical assistance of Pam Fleming. Research on rapid laser heating for device functionality performed as a user project [D.Y., J.L.] through the Functional Hybrid Nanostructures group at the Center for Nanophase Materials Sciences [Z.L., D.S.B., I.I., C.M.R.] which is supported by the U. S. Dept. of Energy Basic Energy Sciences, Division of Scientific User Facilities. Fundamental measurements of nanotube growth [A.A., D.G.] funded by DOE-BES Division of Materials Science.

#### References

1. M.S. Dresselhaus, G. Dresselhaus, P.C. Eklund, *Science of Fullerenes and Carbon Nanotubes* (Academic, San Diego, 1996)
2. J.Q. Lu, T.E. Kopley, N. Moll, D. Roitman, D. Chamberlin, Q. Fu, J. Liu, T.P. Russell, D.A. Rider, I. Manners, M.A. Winnik, *Chem. Mater.* **17**(9), 2227 (2005)
3. J. Gavillet, A. Loiseau, C. Journet, F. Willaime, F. Ducastelle, J.C. Charlier, *Phys. Rev. Lett.* **87**, 275504 (2001)
4. H. Kanzow, A. Ding, *Phys. Rev. B* **60**, 11180 (1999)
5. S. Helveg, C. Lopez-Cartes, J. Sehested, P.L. Hansen, B.S. Clausen, J.R. Rostrup-Nielsen, F. Abild-Oedersen, J.K. Nørskov, *Nature* **427**, 426 (2004)
6. M. Lin, J.P.Y. Tan, C. Boothroyd, K.P. Loh, E.S. Tok, Y. Foo, *Nano Lett.* **6**, 449 (2006)

7. R. Sharma, Z. Iqbal, *Appl. Phys. Lett.* **84**, 990 (2004)
8. A.A. Puzos, D.B. Geohegan, X. Fan, S. Pennycook, *Appl. Phys. Lett.* **76**, 182–184 (2000)
9. D.N. Futaba, K. Hata, T. Yamada, K. Mizuno, M. Yumura, S. Iijima, *Phys. Rev. Lett.* **95**, 056104 (2005)
10. H. Zhu, K. Suenaga, A. Hashimoto, K. Urita, K. Hata, S. Iijima, *Small* **1**, 1180 (2005)
11. S. Huang, X. Cai, J. Liu, *J. Am. Chem. Soc.* **125**, 5636–5637 (2003)
12. Y. Fujiwara, K. Maehashi, Y. Ohno, K. Inoue, K. Matsumoto, *Jpn. J. Appl. Phys.* **44**, 1581 (2005)
13. S.N. Bondi, W.J. Lackey, R.W. Johnson, X. Wang, Z.L. Wang, *Carbon* **44**, 1393 (2006)
14. S. Chiashi, M. Kohno, Y. Takata, S. Maruyama, *J. Phys. Conf. Ser.* **59**, 155 (2007)
15. K. Kaysuya, K. Nagato, Y. Jin, H. Morii, T. Ooi, M. Nakao, *Jpn. J. Appl. Phys.* **46**, L333 (2007)
16. L.X. Zhang, M.J. O'Connell, S.K. Doorn, X.Z. Liao, Y.H. Zhao, E.A. Akhador, M.A. Hoffbauer, B.J. Roop, Q.X. Jia, R.C. Dye, D.E. Peterson, S.M. Huang, J. Liu, Y.T. Zhu, *Nature Mater.* **3**, 673 (2004)
17. A. Jorio, R. Saito, J.H. Hafner, C.M. Lieber, M. Hunter, T. McClure, G. Dresselhaus, M.S. Dresselhaus, *Phys. Rev. Lett.* **86**, 1118 (2001)
18. A.A. Puzos, D.B. Geohegan, S. Jesse, I.N. Ivanov, G. Eres, *Appl. Phys. A* **81**, 223 (2005)
19. R.F. Wood, S. Pannala, J.C. Wells, A.A. Puzos, D.B. Geohegan, *Phys. Rev. B* **75**, 235446 (2007)
20. X. Liu, H. Song, C. Zhou, *Nano Lett.* **6**, 34 (2006)